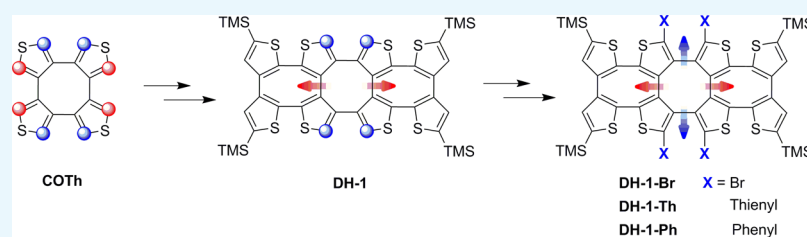# All-Thiophene-Based Double Helix: Synthesis, Crystal Structure, Chiroptical Property and Arylation

Bingbing Li,[†] Sheng Zhang,[†] Lu Li,*,[‡] Zhiying Ma,[†] Chunli Li,[†] Li Xu,[§] and Hua Wang*,[†]

[†]Engineering Research Center for Nanomaterials and [§]College of Chemistry and Chemical Engineering, Henan University, Kaifeng 475004, P. R. China
[‡]School of Chemistry and Chemical Engineering, Shangqiu Normal University, Shangqiu 476000, P. R. China

S *Supporting Information*

ABSTRACT: The all-thiophene-based double helix **DH-1** was designed and prepared originally from the selective deprotonation of cyclooctatetrathiophene (tetra[3,4]thienylene, **COTh**) and following the Negishi coupling reaction with 3,3′-bithiophene. The X-ray crystallographic studies revealed that **DH-1** has a double-helical scaffold. The arylations including tetraphenylation and tetrathienylation were efficiently employed to replace the four α-protons of the central **COTh** of **DH-1** with phenyl and thiophenyl groups via cross-coupling reactions. The chiral resolution of *rac*-**DH-1** was fulfilled via chiral high-performance liquid chromatography, and the chiroptical properties were characterized by circular dichroism spectra and optical rotation. Ultraviolet−visible absorption and fluorescence behaviors of **DH-1** and its arylation products were also characterized to describe the extended conjugated scaffold.

■ INTRODUCTION

Organic double helices are one of the significant species because of their characteristic molecular configurations and extensive applications. Structurally, double helices are constituted of two flexible helical molecular chains which are linked by multiple modes, such as the van der Waals forces,[1] hydrogen bonds,[2] π−π intermolecular interactions,[3] coordinate bonds,[4] and covalent bonds.[5] Among these, covalent bond-linked double helices could exhibit higher stability and could be more practical for applications such as chiral materials and catalysis. As their pioneering work, Rajca[6] and Marsella[7] reported covalent bond-linked double helices on the basis of two tetraphenyl and tetrathienyl chains (Figure 1) in 1997 and 2000, respectively. As the continuation of the work, Wong[8] and Wang[9] extended the helical chains along with the horizontal (one-dimensional) trend recently and obtained two longest double helices, which contain two hexaphenyl and hexathienyl chains (Figure 1), respectively. However, the two-dimensional cross-derivatization of the double helices have been rarely reported. One of the main reasons is that the reported double helices including tetra- and hexa-aryl double helices do not have applicable active Ar−H for further vertical derivatization.

In our previous work, the high selectivity for ipsilateral deprotonation of **COTh** was studied, and a stepwise lithiation procedure was proved.[9,10] For utilizing this selective deprotonation, three one-dimensional double-helical shaped
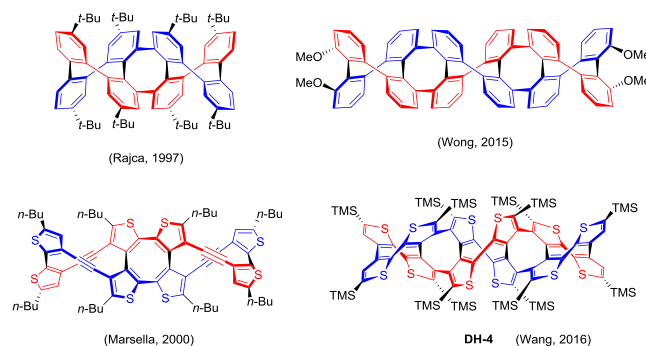

Figure 1. Molecular structures of covalent bond-linked double helices based on phenyl and thienyl chains.

oligothiophenes were synthesized (Figure 2).[9] Meanwhile, a systematic synthetic strategy of one-dimensional oligothiophenes based on the selective deprotonation of **COTh** was emploed. As the extension to these amazing works, herein, we have designed and synthesized a novel one-dimensional thiophene-based double helix (**DH-1**) by the Negishi coupling reaction between bithiophene and **COTh**. **DH-1** has four active α-H on the central **COTh** unit for further two-
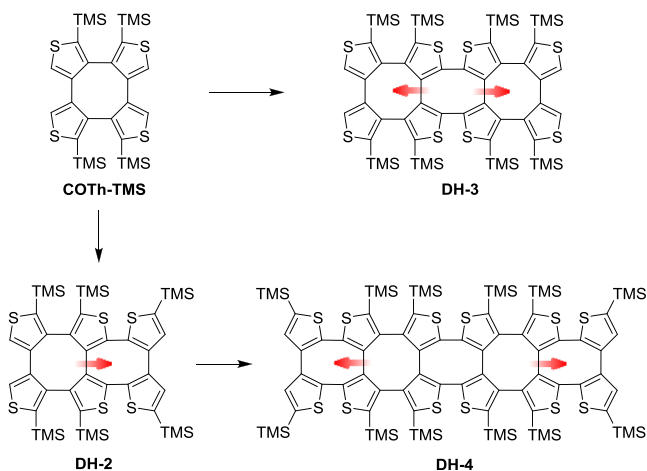
Figure 2. Reported double helices, the horizontal derivatives from **COTh**−**TMS**, as building blocks.

dimensional derivatization. Besides the efficient chiral resolution of **DH-1**, the tetrabromination and tetra-arylation have effectively occurred at the central **COTh** unit of **DH-1** (Figure 3). Furthermore, the crystal structure of **DH-1** and the spectroscopic properties of **DH-1** and its aryl derivatives are also described.

■ RESULTS AND DISCUSSION

Syntheses of DH-1 and Its Arylation. There are two synthetic routes to **DH-1**. According to the ipsilateral selectivity of deprotonation of **COTh** in the presence of *n*-BuLi in tetrahydrofuran (THF),[9,10] the obtained tetralithiated intermediate was converted to an aryl zinc intermediate in Route-A (Scheme 1) for a further Negishi reaction with 2,2′-dibromo-5,5′-bistrimethylsilanyl[3,3′]bithiophenyl (**BTBT**) at 120 °C. Such a palladium-catalyzed cross-coupling generated **DH-1** in a low yield of 10%. The low yield might be from the steric hindrance of two ZnCl groups and the weak activity of the C−Br bond of **BTBT** in the Negishi reaction.

To avoid the adverse factors and increase the reaction yield, the Negishi reagent was changed from the **COTh** zinc intermediate to the **BTBT** zinc intermediate and then reacted with **COTh**−**I**[10] (Route-B, Scheme 1). Under the same palladium-catalyzed reaction conditions as shown in Route-A, the yield of **DH-1** was enhanced from 10% to 35%. The improvement of the synthetic yield may be attributed to the higher reactivity of the C−I bond from the aryl iodide.

Arylation of **DH-1** is very important to the double helix, so that the functionalized derivatives may be employed in some fields, such as opt-electric materials, supermolecular chemistry, and so on. The big challenge is in the organic synthesis itself because of the activity of the four α-H on the central **COTh**

unit of **DH-1** and the steric hindrance for bond formation. In our case, **DH-1** was first treated with *n*-BuLi in THF at −78 °C. After the deprotonation at 60 °C for 2 h and the following quenching with 1,2-dibromotetrachloroethane, **DH-1**−**Br** was obtained in 80% yield (Scheme 1). The respective results indicate that α-H on the central **COTh** unit of **DH-1** have enough activity for deprotonation, which is helpful for further vertical derivatization.

The tetrathienylation of **DH-1** took place between the organozinc intermediate prepared from tetradeprotonated **DH-1** and 3-bromothiophene in the presence of Pd(PPh₃)₄. Such a coupling reaction generated **DH-1**−**Th** in a yield of 26%. Besides the Negishi coupling, Suzuki reaction was also employed for tetraphenylation. The reaction of **DH-1**−**Br** and phenylboronic acid in the presence of CsCO₃ and Pd(PPh₃)₄ was performed, and the target product **DH-1**−**Ph** was yielded in 34% (Scheme 1).

With the good successes of bromination and arylation of **DH-1**, a more synthetic challenging work for making a cross-double helix, **DH-5**, is of high interest to us because of its cross-dimensional double-helical configuration. Referred to the reaction conditions of thienylation and phenylation of **DH-1**, two approaches (Route-A and Route-B, Scheme 2) from **DH-1** and **DH-1**−**Br** under the conditions of Negishi reaction were employed to synthesize **DH-5**. Unfortunately, **DH-5** has not been produced after many attempts by changing the reaction conditions. One of the possible reasons is the torsional strain of the double-helical skeleton, which may be too huge to lead the harsh building of the new vertical **COTh**s.

X-ray Crystal Structure Analyses of DH-1. The single crystal of **DH-1** was obtained by slow evaporation from the chloroform/methanol (1:3, v/v) solution. Its crystal belongs to the triclinic space group $P\bar{1}$. The crystal structure of **DH-1** is shown in Figure 4a, from which the double-helical molecular configuration can be visualized. Similar to the reported **DH-3**,[9] **DH-1** has three **COTh** moieties, which are sequentially annelated together in the molecule, and the two quadruple thiophene chains are intertwined with each other via the C−C single bonds. Different from the case of **DH-3**, which has one tetra[2,3]thienylene and two tetra[3,4]thienylene,[9] however, **DH-1** shows an alternation of two tetra[2,3]thienylene and one tetra[3,4]thienylene. Additionally, the molecular length of **DH-1** is 12.325 Å (C5···C22), which is longer than that of **DH-3** (11.921 Å). Simultaneously, the average value of the dihedral angles of the two terminal thiophene rings of each strand in the double-helical oligomer is decreased from 196° of **DH-3** to 168° of **DH-1**. These correlative changes are due to the twist degree of the **COTh** core of each double helix, which is influenced by the steric hindrance of the introduced TMS groups.

Figure 4b shows the packing of **DH-1**. Two pairs of enantiomers are stacked in a unit cell. Multiple interactions
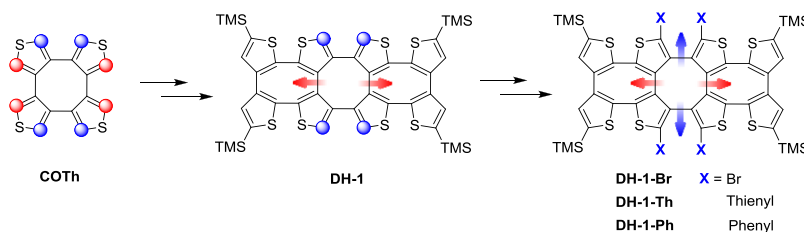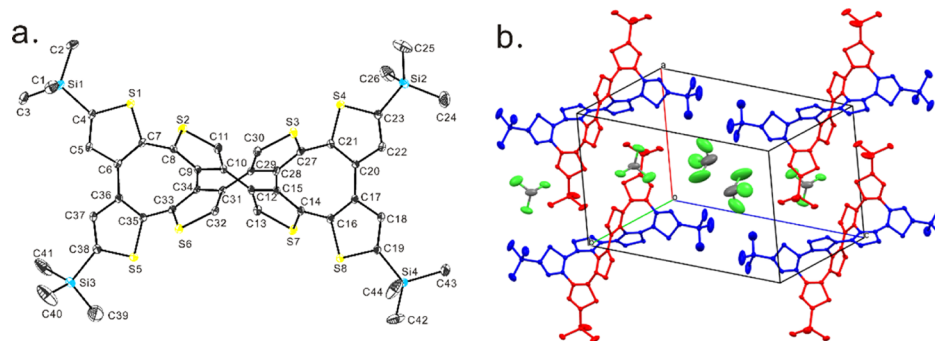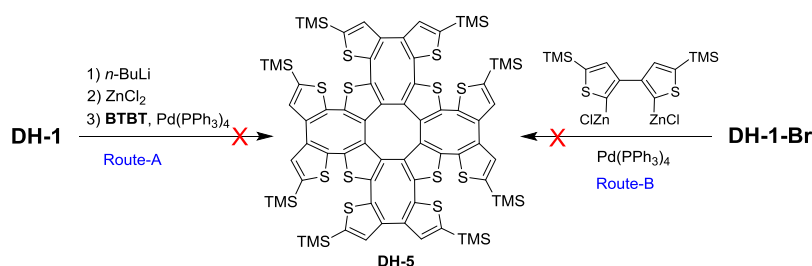

Figure 3. Molecular structures of the target double helix (**DH-1**) and its two-dimensional derivatives.

Scheme 1. Synthetic Routes to DH-1 and Its Aryl Derivatives
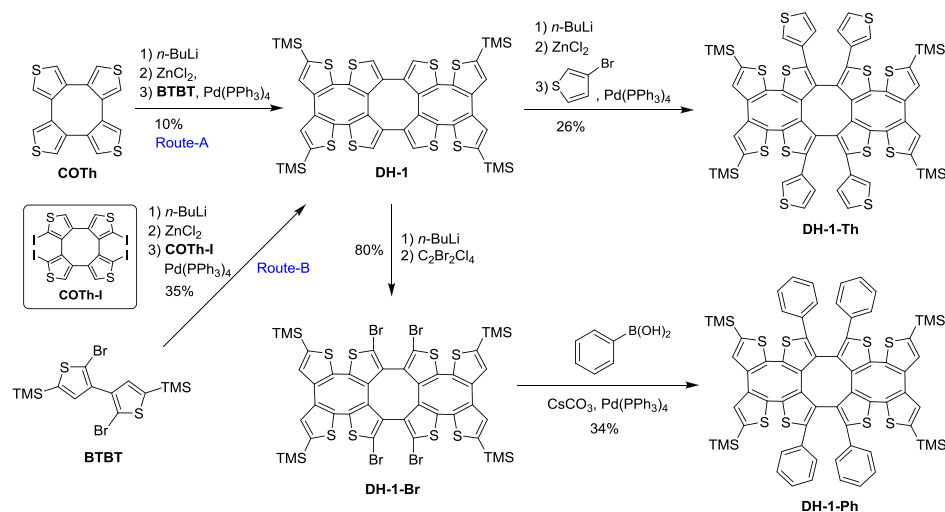
**Scheme 2. Unsuccessful Synthetic Routes to DH-5**

Figure 4. X-ray crystal structures (a) and crystal packing (b) of **DH-1**. Carbon, silicon, sulfur, and chlorine atoms are depicted with the thermal ellipsoids set at the 30% probability level. All hydrogen atoms are omitted for clarity.

between the molecules of the CHCl₃ solvent and the molecules of **DH-1** lend the molecular arrangements, such as Cl3···C18 (3.421 Å), Cl4···H24C (2.848 Å), H46A···S1 (2.892 Å), and H46A···H2B (2.358 Å). It is clear that the CHCl₃ solvent shows an important factor for the formation of the **DH-1** crystal.

Resolution of Double Helix rac-DH-1 and the Chiroptical Properties. The resolution of *rac-DH-1* was carried out by chiral high-performance liquid chromatography, with *n*-hexane/isopropanol (99.5:0.5, v/v) as the eluent. The two enantiomers were obtained on a semipreparative-scale chiral column (Figure S17, Supporting Information). From the 5 mg scale of *rac-DH-1*, 2.1 mg (ee = 84%) of (+)-**DH-1** and 1.2 mg (ee = 89%) of (−)-**DH-1** were obtained. The optical rotations of (+)-**DH-1**, $[\alpha]_D^{23} = +200°$ (*c* = 0.0013 g/mL in dichloromethane) and (−)-**DH-1**, $[\alpha]_D^{23} = -210°$ (*c* = 0.0013

g/mL in dichloromethane) were observed, respectively. The circular dichroism (CD) spectra of (+)-**DH-1** and (−)-**DH-1** were taken in dichloromethane. Two enantiomers, (+)-**DH-1** and (−)-**DH-1**, show nearly identical symmetric image spectra (Figure 5).

Electronic Absorption Spectra of DH-1 and the Arylation Products. The ultraviolet−visible (UV−vis) absorption spectra of **DH-1**, **DH-1−Th**, and **DH-1−Ph** in dichloromethane are shown in Figure 6a. **DH-1** has two major absorption peaks at 231 and 282 nm and a weak absorption band peaked at 344 nm. In the absorption spectra of **DH-1−Th**, the introduction of thienyl leads the major absorption peaks bathochromic-shifted to 239 and 286 nm compared with the case of **DH-1**. In the case of **DH-1−Ph**, its absorption behavior is very similar to that of **DH-1−Th**. Compared with the case of **DH-1**, **DH-1−Ph** and **DH-1−Th** show high
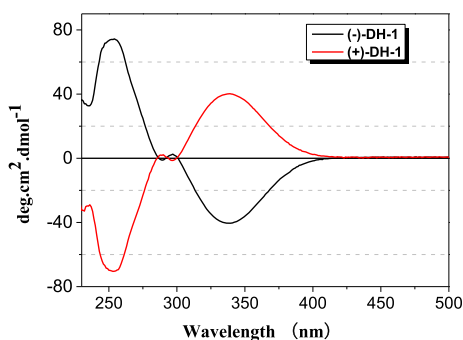
Figure 5. CD spectra of (−)-**DH-1** (black line, ee = 89%, 1.4 × 10⁻⁵ M in dichloromethane) and (+)-**DH-1** (red line, ee = 84%, 1.4 × 10⁻⁵ M in dichloromethane) at room temperature.

intensity and broad absorption band in the long-wavelength region. Such spectroscopic behaviors are attributed to the extended conjugations of **DH-1−Ph** and **DH-1−Th**. Meanwhile, the phenyl groups and thiophenyl groups show conjugation effects similar to that of **DH-1** because of their twist configurations in the molecules of **DH-1−Ph** and **DH-1−Th**.

The fluorescence behaviors of **DH-1**, **DH-1−Ph,** and **DH-1−Th** in dichloromethane are also characterized. As shown in Figure 6b, **DH-1** shows a much strong emission peaked at 457 nm. Compared with the case of **DH-1**, **DH-1−Ph** and **DH-1−Th** exhibit a much weak emission, and their emission peaks are bathochromic-shifted to 525 and 516 nm, respectively. The obvious bathochromic shifts of emission are attributed to the increased conjugation extension of **DH-1−Ph** and **DH-1−Th**. The single bond rotation between the aryl groups and the central **COTh** unit might be the main reason for the increase in the nonradiative deactivation processes and decrease in the intensity of emission.

Theoretical Calculations for Electronic Absorption Spectra of DH-1 and the Arylation Products. To obtain the effects of molecular structure and electronic structure on the spectroscopic properties of **DH-1** and its derivatives, their electronic structures and excited-state calculations were performed by density functional theory (DFT) and time-dependent DFT calculations using Gaussian 09 program package.[11] The geometries were fully optimized at the B3LYP/6-31G* level of theory.[12] Subsequently, frequency analysis was also performed at the same level of theory to ensure that the structures correspond to a true minimum. On the basis of the optimized geometries, the excited-state calculations were performed by using the MPW1B95 func-

tional[13] and the polarizable continuum model[14] at the 6-31G* level. As depicted in Figure S18 (Supporting Information) and Figure 6a, the shapes and positions of absorption peaks (listed in Table S2, Supporting Information) from the predicted UV− vis spectra were consistent with the experimental curves. The excitation energies, oscillator strengths, and transition contributions of the most important states are listed in Table S2. In the predicted UV−vis spectrum of **DH-1**, the two major absorption peaks located at 231 and 282 nm were in agreement with the experimental results. Further, the largest contributions to the major absorption peaks were attributed to $S_0 \rightarrow S_{37}$ and $S_0 \rightarrow S_7$, respectively. The lowest energy absorption band of **DH-1** was associated to the $S_0 \rightarrow S_2$ transition, which was dominated by the highest occupied molecular orbital (HOMO) − 1 → lowest occupied molecular orbital (LUMO) + 1 and HOMO → LUMO transitions. Compared with **DH-1**, there were slight bathochromic shifts for the values of the two major absorption peaks in the spectra of **DH-1−Ph** and **DH-1−Th**. Further, the high-intensity absorption bands in the long-wavelength region in **DH-1−Ph** and **DH-1−Th** were attributed to the large transition dipole moments between S_0 and S_2, as listed in Table S2.

■ CONCLUSIONS

In summary, we have explored the efficient synthesis of the all-thiophene-based double helix, **DH-1**, and studied its crystal structure, chiral resolution, and chiroptical property. Such covalent bond-linked double helices could be more practical for applications such as chiral materials and catalysis after functionalization. Furthermore, bromination and arylation efficiently occur at the four active α-positions on the central **COTh** unit of **DH-1**, which means **DH-1** is a potential candidate for making the amazing two-dimensional cross-double helix, **DH-5**. It has been proved in our current work that making **DH-5** is a huge challenge, but the attempts have not been given up in our lab.

■ EXPERIMENTAL SECTION

General Procedures and Materials. THF was freshly distilled from sodium/benzophenone prior to use. The compound **BTBT** was prepared according to our previous research work.[15] The concentration of *n*-BuLi (in hexane) was determined by titration with *N*-pivaloyl-*o*-toluidine.[16] Silica gel (300−400 mesh) was employed for column chromatography. Analytical thin-layer chromatography was performed on glass plates of silica gel GF-254 with UV detection. The standard techniques for synthesis under an inert atmosphere, using gasbag and Schlenk glassware equipped with an 8 mm
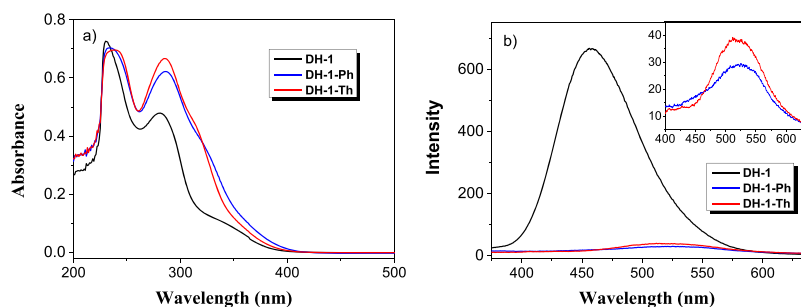
Figure 6. (a) UV−vis spectra of **DH-1**, **DH-1−Ph**, and **DH-1−Th** in dichloromethane ([C] = 1 × 10⁻⁵ M). (b) Fluorescence spectra of **DH-1**, **DH-1−Ph**, and **DH-1−Th** in dichloromethane ([C] = 1 × 10⁻⁵ M), λ_{ex} = 330 nm, slit: 5/5.

polytetrafluoroethylene vacuum stopcock, were employed. All starting materials and reagents were commercially available. The two enantiomers (+)-**DH-1** and (−)-**DH-1** were obtained on a semipreparative-scale chiral column (RC-SCDP5).

The proton nuclear magnetic resonance (^1H NMR) and carbon (^{13}C) NMR spectra were recorded on a 400 MHz NMR instrument using $CDCl_3$ as the solvent. The IR spectra were obtained using a Fourier transform infrared instrument. High-resolution mass spectrometry (HRMS) analysis was carried out on a mass spectrometer equipped with an FTMS and LTQ FT Ultra. The melting point was determined on a Melt-Temp apparatus and was uncorrected. A slow evaporation of the solutions of **DH-1** in $CHCl_3$–CH_3OH (1:3, v/v) was employed for growing single crystals. The X-ray crystallographic analysis was performed using the crystal of **DH-1** with the size 0.33 × 0.21 × 0.17 mm^3. The intensity data were collected with the ω scan mode (296 K) on a diffractometer with a CCD detector using Mo Kα radiation (λ = 0.71073 Å). The data were corrected for Lorentz and polarization effects, and the absorption corrections were performed using the SADABS program.[17] The crystal structures were solved using the SHELXTL program and refined using full-matrix least-squares.[18] Further details are deposited in the CIFs (see the Supporting Information).

Synthesis of DH-1. *Method A.* To a solution of **COTh** (104 mg, 0.32 mmol) in dry THF (8 mL), n-BuLi (0.58 mL, 2.33 M in hexane, 1.35 mmol, 4.5 equiv) was added dropwise at −78 °C. The reaction temperature was allowed to warm to room temperature and then was heated to 60 °C. After 2 h, $ZnCl_2$ (205 mg, 1.5 mmol, 5.0 equiv) was added at −78 °C, and then the reaction mixture was warmed to room temperature. The prepared organozinc was added to the mixture of **BTBT** (282 mg, 0.60 mmol, 2.0 equiv), $Pd(PPh_3)_4$ (35 mg, 0.03 mmol, 0.1 equiv), and THF (5 mL) in a glovebox. The reaction mixture was heated to 120 °C for 48 h and was quenched with methanol at 0 °C. The mixture was extracted with CH_2Cl_2 (3 × 10 mL) and then washed with saturated NaCl (10 mL) and water (2 × 10 mL). After the mixture dried over $MgSO_4$, the solvent was removed under vacuum. The residue was purified by column chromatography on silica gel with petrol ether (60−90 °C)/$CHCl_3$ (4/1) as a white solid to yield **DH-1** (28 mg, 10%). mp: >300 °C. ^1H NMR ($CDCl_3$, 400 MHz): δ (ppm) 7.21 (s, 4 H), 7.09 (s, 4 H), 0.34 (s, 36 H). ^{13}C NMR (100 MHz, $CDCl_3$): δ 142.31, 138.53, 138.47, 137.59, 136.28, 135.19, 133.53, 126.98, 0.02. MS (EI, 70 eV) *m/z*: 922.16 [M$^+$]. HRMS (MALDI MS EI$^+$) *m/z*: calcd for [$C_{44}H_{44}Si_4S_8^+$], 940.0286; found, 940.0280. IR (KBr): 2954 cm^{-1} (C−H).

Method B. To a solution of **BTBT** (105 mg, 0.22 mmol) in dry THF (10 mL), n-BuLi (0.19 mL, 2.4 M in hexane, 0.46 mmol, 2.05 equiv) was added dropwise at −78 °C. After the temperature was maintained at −78 °C for 2 h, $ZnCl_2$ (64 mg, 0.47 mmol, 2.1 equiv) was added at −78 °C, and the reaction temperature was warmed to room temperature. The prepared organozinc was added to the mixture of **COTh−I** (281.6 mg, 0.60 mmol, 2.0 equiv), $Pd(PPh_3)_4$ (25 mg, 0.02 mmol, 0.1 equiv), and THF (5 mL) in a glovebox. The reaction mixture was heated to 120 °C for 48 h and was quenched with methanol at 0 °C. The mixture was extracted with CH_2Cl_2 (3 × 10 mL) and then washed with saturated NaCl (10 mL) and water (2 × 10 mL). After the mixture dried over $MgSO_4$, the solvent was removed under vacuum. The residue was purified by column chromatography on silica gel with petrol ether (60−

90 °C)/CH_2Cl_2 (5/1) as a white solid to yield **DH-1** (28.3 mg, 35%).

Synthesis of DH-1−Br. To a solution of **DH-1** (35 mg, 0.04 mmol) in dry THF (15 mL), n-BuLi (0.06 mL, 2.4 M in hexane, 0.15 mmol, 4.1 equiv) was added dropwise at −78 °C. The reaction temperature was allowed to warm to room temperature and then was heated to 60 °C. After 2 h, $C_2Br_2Cl_4$ (50 mg, 0.15 mmol, 4.1 equiv) was added at −78 °C, and then the reaction mixture was slowly warmed to room temperature overnight. The mixture was quenched with methanol at 0 °C, extracted with CH_2Cl_2 (3 × 10 mL), and then washed with saturated NaCl (10 mL) and water (2 × 10 mL). After the mixture dried over $MgSO_4$, the solvent was removed under vacuum. The residue was purified by column chromatography on silica gel with petrol ether (60−90 °C)/$CHCl_3$ (4/1) as a white solid to yield **DH-1−Br** (37 mg, 80%). mp: >300 °C. ^1H NMR ($CDCl_3$, 400 MHz): δ (ppm) 7.07 (s, 4 H), 0.34 (s, 36 H). ^{13}C NMR (100 MHz, $CDCl_3$): δ 143.34, 136.39, 1350.82, 135.62, 135.02, 133.95, 115.88, −0.01. HRMS (ESI) *m/z*: calcd for [$C_{44}H_{41}Br_4Si_4S_8^+$], 1252.6779; found, 1252.6848. IR (KBr): 2953 cm^{-1} (C−H).

Synthesis of DH-1−Th. To a solution of **DH-1** (20 mg, 0.21 mmol) in dry THF (10 mL), n-BuLi (0.04 mL, 2.5 M in hexane, 0.1 mmol, 4.5 equiv) was added dropwise at −78 °C. The reaction temperature was allowed to warm to room temperature and then was heated to 60 °C. After 2 h, $ZnCl_2$ (14.5 mg, 0.11 mmol, 5.0 equiv) was added at −78 °C, and then the reaction mixture was warmed to room temperature. The prepared organozinc was added to the mixture of 3-bromothiophene (17 mg, 0.11 mmol, 5.0 equiv), $Pd(PPh_3)_4$ (2.5 mg, 0.02 mmol, 0.1 equiv), and THF (5 mL) in a glovebox. The reaction mixture was heated to 120 °C for 48 h and was quenched with methanol at 0 °C. The mixture was extracted with CH_2Cl_2 (3 × 10 mL) and then washed with saturated NaCl (10 mL) and water (2 × 10 mL). After the mixture dried over $MgSO_4$, the solvent was removed under vacuum. The residue was purified by column chromatography on silica gel with petrol ether (60−90 °C)/CH_2Cl_2 (5/1) as a white solid to yield **DH-1−Th** (7 mg, 26%). mp: >300 °C. ^1H NMR ($CDCl_3$, 400 MHz): δ (ppm) 7.20 (s, 4H), 6.84 (dd, J = 5.0, 3.0 Hz, 4H), 6.50 (dd, J = 2.9, 1.1 Hz, 4H), 6.39 (dd, J = 5.0, 1.1 Hz, 4H), 0.37 (s, 36H). ^{13}C NMR (100 MHz, $CDCl_3$): δ 144.49, 142.53, 138.84, 138.68, 137.41, 136.28, 133.60, 133.43, 131.53, 128.61, 127.79, 127.11, 0.05. HRMS (ESI) *m/z*: calcd for [$C_{60}H_{53}Si_4S_{12}^+$], 1268.9867; found, 1268.9887. IR (KBr): 2955 cm^{-1} (C−H).

Synthesis of DH-1−Ph. The mixture of **DH-1−Br** (24 mg, 0.02 mmol), phenylboronic acid (12.3 mg, 0.1 mmol, 5 equiv), $Pd(PPh_3)_4$ (9 mg, 0.008 mmol, 0.4 equiv), and Cs_2CO_3 (65 mg, 0.2 mmol, 10 equiv) in THF (10 mL) and degassed H_2O (0.2 mL) was heated to 100 °C. The mixture was extracted with CH_2Cl_2 (3 × 10 mL) and then washed with saturated NaCl (10 mL) and water (2 × 10 mL). After the mixture dried over $MgSO_4$, the solvent was removed under vacuum. The residue was purified by column chromatography on silica gel with petrol ether (60−90 °C)/CH_2Cl_2 (5/1) as a white solid to yield **DH-1−Ph** (9 mg, 34%). mp >300 °C. ^1H NMR ($CDCl_3$, 400 MHz): δ (ppm) 7.24 (s, 1H), 7.00 (t, J = 7.4 Hz, 1H), 6.79 (t, J = 7.7 Hz, 2H), 6.56 (d, J = 7.5 Hz, 2H), 0.39 (s, 8H). ^{13}C NMR (100 MHz, $CDCl_3$): δ 142.74, 139.05, 138.79, 138.01, 137.14, 136.29, 133.95, 132.88, 130.85, 127.04, 124.75, 122.07, 0.02. HRMS (ESI) *m/z*: calcd for

$[C_{68}H_{61}Si_4S_8{}^+]$, 1245.1611; found, 1245.1615. IR (KBr): 2955 cm^{-1} (C−H).

■ ASSOCIATED CONTENT

Ⓢ Supporting Information

The Supporting Information is available free of charge on the ACS Publications website at DOI: 10.1021/acsomega.8b02492.

Experimental procedures and characterization data for all compounds (CIF)

Experimental procedures and characterization data for all compounds NMR, HRMS, and IR spectra of **DH-1**, **DH-1−Br**, **DH-1−Ph**, **DH-1−Th**; CIF of *rac*-**DH-1**; and calculated absorption spectra of **DH-1**, **DH-1−Ph**, and **DH-1−Th** in dichloromethane solution using TDDFT/PCM approaches (PDF)

■ AUTHOR INFORMATION

Corresponding Authors
*E-mail: sqlilu@163.com (L.L.).
*E-mail: hwang@henu.edu.cn (H.W.).

ORCID Ⓞ
Chunli Li: 0000-0003-0707-2800
Hua Wang: 0000-0003-3239-1600

Notes
The authors declare no competing financial interest.

■ ACKNOWLEDGMENTS

■ REFERENCES

(1) (a) Schomaker, E.; Challa, G. Complexation of stereoregular poly (methyl methacrylates). 14. The basic structure of the stereocomplex of isotactic and syndiotactic poly (methyl methacrylate). *Macromolecules* **1989**, *22*, 3337−3341. (b) Kumaki, J.; Kawauchi, T.; Yashima, E. Two-dimensional folded chain crystals of a synthetic polymer in a Langmuir-Blodgett film. *J. Am. Chem. Soc.* **2005**, *127*, 5788−5789. (c) Kumaki, J.; Kawauchi, T.; Okoshi, K.; Kusanagi, H.; Yashima, E. Supramolecular helical structure of the stereocomplex composed of complementary isotactic and syndiotactic poly (methyl methacrylates) as revealed by atomic force microscopy. *Angew. Chem., Int. Ed.* **2007**, *46*, 5348−5351.

(2) (a) Tanaka, Y.; Katagiri, H.; Furusho, Y.; Yashima, E. A modular strategy to artificial double helices. *Angew. Chem., Int. Ed.* **2005**, *44*, 3867−3870. (b) Ito, H.; Ikeda, M.; Hasegawa, T.; Furusho, Y.; Yashima, E. Synthesis of complementary double-stranded helical oligomers through chiral and achiral amidinium-carboxylate salt bridges and chiral amplification in their double-helix formation. *J. Am. Chem. Soc.* **2011**, *133*, 3419−3432. (c) Hasegawa, T.; Furusho, Y.; Katagiri, H.; Yashima, E. Enantioselective synthesis of complementary double-helical molecules that catalyze asymmetric reactions. *Angew. Chem., Int. Ed.* **2007**, *46*, 5885−5888. (d) Miwa, K.; Furusho, Y.; Yashima, E. Ion-triggered spring-like motion of a double helicate accompanied by anisotropic twisting. *Nat. Chem.* **2010**, *2*, 444−449. (e) Li, J.; Wisner, J. A.; Jennings, M. C. A self-associating ADADA hydrogen-bonded double helix. *Org. Lett.* **2007**, *9*, 3267−3269.

(3) (a) Berl, V.; Huc, I.; Khoury, R. G.; Krische, M. J.; Lehn, J.-M. Interconversion of single and double helices formed from synthetic molecular strands. *Nature* **2000**, *407*, 720−723. (b) Berl, V.; Huc, I.; Khoury, R. G.; Lehn, J.-M. Helical molecular programming: supramolecular double helices by dimerization of helical oligopyridine-dicarboxamide strands. *Chem.—Eur. J.* **2001**, *7*, 2810−2820.

(4) (a) Lehn, J. M.; Rigault, A.; Siegel, J.; Harrowfield, J.; Chevrier, B.; Moras, D. Spontaneous assembly of double-stranded helicates from oligobipyridine ligands and copper (I) cations: structure of an inorganic double helix. *Proc. Natl. Acad. Sci. U.S.A.* **1987**, *84*, 2565−2569. (b) Lehn, J.-M.; Rigault, A. Helicates: tetra- and pentanuclear double helix complexes of CuI and poly (bipyridine) strands. *Angew. Chem., Int. Ed. Engl.* **1988**, *27*, 1095−1097. (c) Hasenknopf, B.; Lehn, J.-M.; Kneisel, B. O.; Baum, G.; Fenske, D. Self-assembly of a circular double helicate. *Angew. Chem., Int. Ed. Engl.* **1996**, *35*, 1838−1840. (d) Hasenknopf, B.; Lehn, J. M.; Baum, G.; Fenske, D. Self-assembly of a heteroduplex helicate from two different ligand strands and Cu(II) cations. *Proc. Natl. Acad. Sci. U.S.A.* **1996**, *93*, 1397−1400. (e) Hasenknopf, B.; Lehn, J.-M.; Kneisel, B. O.; Baum, G.; Fenske, D. Self-assembly of a circular double helicate. *Angew. Chem., Int. Ed. Engl.* **1996**, *35*, 1838−1840.

(5) (a) Mascal, M.; Wood, I. G.; Begley, M. J.; Batsanov, A. S.; Walsgrove, T.; Slawin, A. M. Z.; Williams, D. J.; Drake, A. F.; Siligardi, G. Indole-fused tetraazacyclooctadecanes: double-helical macrocycles. *J. Chem. Soc., Perkin Trans. 1* **1996**, 2427−2433. (b) An, D. L.; Nakano, T.; Orita, A.; Otera, J. Enantiopure double-helical alkynyl cyclophanes. *Angew. Chem., Int. Ed.* **2002**, *41*, 171−173. (c) Nakatani, Y.; Furusho, Y.; Yashima, E. Synthesis of helically twisted [1+1]-macrocycles assisted by amidinium-carboxylate salt bridges and control of their chiroptical properties. *Org. Biomol. Chem.* **2013**, *11*, 1614−1623.

(6) Rajca, A.; Safronov, A.; Rajca, S.; Shoemaker, R. Double helical octaphenylene. *Angew. Chem., Int. Ed. Engl.* **1997**, *36*, 488−491.

(7) Marsella, M. J.; Kim, I. T.; Tham, F. Toward conjugated double helical ladder polymers: cyclooctatetrathiophene as a highly versatile double helical scaffold. *J. Am. Chem. Soc.* **2000**, *122*, 974−975.

(8) Chen, J.-X.; Han, J.-W.; Wong, H. N. C. Synthesis and Chiroptical Properties of Double-Helical (M)- and (P)-o-Oligophenylenes. *Org. Lett.* **2015**, *17*, 4296−4299.

(9) Zhang, S.; Liu, X.; Li, C.; Li, L.; Song, J.; Shi, J.; Morton, M.; Rajca, S.; Rajca, A.; Wang, H. Thiophene-Based Double Helices: Syntheses, X-ray Structures, and Chiroptical Properties. *J. Am. Chem. Soc.* **2016**, *138*, 10002−10010.

(10) Li, L.; Li, B.; Li, C.; Ma, Z.; Xu, L.; Wang, H. Selective deprotonation of tetra[3,4]thienylene in the presence of n-BuLi. *Org. Chem. Front.* **2017**, *4*, 1019−1023.

(11) Frisch, M. J.; Trucks, G. W.; Schlegel, H. B.; Scuseria, G. E.; Robb, M. A.; Cheeseman, J. R.; Scalmani, G.; Barone, V.; Mennucci, B.; Petersson, G. A.; Nakatsuji, H.; Caricato, M.; Li, X.; Hratchian, H. P.; Izmaylov, A. F.; Bloino, J.; Zheng, G.; Sonnenberg, J. L.; Hada, M.; Ehara, M.; Toyota, K.; Fukuda, R.; Hasegawa, J.; Ishida, M.; Nakajima, T.; Honda, Y.; Kitao, O.; Nakai, H.; Vreven, T.; Montgomery, J. A., Jr.; Peralta, J. E.; Ogliaro, F.; Bearpark, M.; Heyd, J. J.; Brothers, E.; Kudin, K. N.; Staroverov, V. N.; Kobayashi, R.; Normand, J.; Raghavachari, K.; Rendell, A.; Burant, J. C.; Iyengar, S. S.; Tomasi, J.; Cossi, M.; Rega, N.; Millam, J. M.; Klene, M.; Knox, J. E.; Cross, J. B.; Bakken, V.; Adamo, C.; Jaramillo, J.; Gomperts, R.; Stratmann, R. E.; Yazyev, O.; Austin, A. J.; Cammi, R.; Pomelli, C.; Ochterski, J. W.; Martin, R. L.; Morokuma, K.; Zakrzewski, V. G.; Voth, G. A.; Salvador, P.; Dannenberg, J. J.; Dapprich, S.; Daniels, A. D.; Farkas, O.; Foresman, J. B.; Ortiz, J. V.; Cioslowski, J.; Fox, D. J. *Gaussian 09*, D.01; Gaussian, Inc.: Wallingford, CT, 2013.

(12) Stephens, P. J.; Devlin, F. J.; Chabalowski, C. F.; Frisch, M. J. Ab Initio Calculation of Vibrational Absorption and Circular Dichroism Spectra Using Density Functional Force Fields. *J. Phys. Chem.* **1994**, *98*, 11623−11627.

(13) Zhao, Y.; Truhlar, D. G. Hybrid Meta Density Functional Theory Methods for Thermochemistry, Thermochemical Kinetics, and Noncovalent Interactions: The MPW1B95 and MPWB1K Models and Comparative Assessments for Hydrogen Bonding and van der Waals Interactions. *J. Phys. Chem. A* **2004**, *108*, 6908−6918.

(14) Scalmani, G.; Frisch, M. J. Continuous surface charge polarizable continuum models of solvation. I. General formalism. *J. Chem. Phys.* **2010**, *132*, 114110−114124.

(15) Wang, Y.; Wang, Z.; Zhao, D.; Wang, Z.; Cheng, Y.; Wang, H. Efficient Synthesis of Trimethylsilyl-Substituted Dithieno[2,3-b:3′,2′-d]thiophene, Tetra[2,3-thienylene] and Hexa[2,3-thienylene] from Substituted [3,3′]Bithiophenyl. *Synlett* **2007**, 2390−2394.

(16) Suffert, J. Simple direct titration of organolithium reagents using N-pivaloyl-o-toluidine and/or N-pivaloyl-o-benzylaniline. *J. Org. Chem.* **1989**, *54*, 509−510.

(17) Sheldrick, G. M. *SADABS*; University of Gottingen: Germany, 1996.

(18) Sheldrick, G. M. *SHELXTL*, version 5.1; Bruker Analytical X-ray Systems, Inc.: Madison, WI, 1997.